RSC Advances

ROYAL SOCIETY OF CHEMISTRY

www.rsc.org/advances

Fractals in carbon nanotube buckypapers

Chunyong Zhang [a], Haiyan Cui [a] , Zhenzhu He [a], Lin Su [b] , Degang Fu [b]*

a. Department of Chemistry, College of Science, Nanjing Agricultural University, Nanjing 210095, China

b . State Key Laboratory of Bioelectronics, Southeast University, Nanjing 210096, China

Paper submitted for publication in *RSC Advances*

* Corresponding Author: Dr. Chunyong Zhang, Tel: +86 25 84395207, Fax: +86 25 84395207

E-mail： zhangchy@njau.edu.cn

ABSTRACT

Here, the fractal properties of buckypapers (BPs) have been initially studied by SEM imaging at different scales, as well as by low-pressure nitrogen adsorption analysis. The BPs under investigation are composed of either single-walled carbon nanotubes (SWNTs) or multi-walled carbon nanotubes (MWNTs). Fractal analysis of either film morphology or adsorption isotherm shows that the fractal dimension of SWNT-BPs is higher than that of the MWNT-BPs. As a result, such difference offers a new and important explanation for their differing adsorption capabilities during decontamination processes.

KEYWORDS

carbon nanotube; buckypaper; fractal analysis; adsorption; nitrogen adsorption analysis

1. Introduction

In recent years, carbon nanotubes (CNTs) have attracted considerable interest for their unique structures and fascinating properties.[1,2] As a consequence, they have been applied to many important fields, such as material, electronics, energy and environment. Specifically, CNTs are fast becoming ideal candidates for use in wastewater treatment because of their excellent adsorption capability.[3-5] As is known, CNTs can be manufactured in the form of single-walled carbon nanotubes (SWNTs) or multi-walled carbon nanotubes (MWNTs), distinguished by the number of graphite layers. Interestingly, due to the different microstructures and BET surface areas, the adsorption capability of SWNTs is proved to be much higher than that of MWNTs.[6]

However, in adsorption processes, CNTs are generally applied in the form of powder suspended in aqueous solutions. The inconvenience of this kind of approach lies in the separation step at the end of

operation.[7] Alternatively, buckypapers (BPs) makes handling CNTs easy in many correlative experiments. BPs are free-standing films of CNTs prepared by filtration, which are characterized by their unique mesoporous structures.[8] It has been demonstrated that the nature of CNTs strongly influences the performance of BPs. Previous experimental works showed that BPs made of SMNTs and MWNTs (i.e. SWNT-BPs and MWNT-BPs) exhibited quite different surface morphology and mechanical property.[9,10] Unfortunately, to experimentally extract the microstructure from BPs remains to be a challenging task - new techniques or methods are needed. Thus, a novel mathematical tool named fractal geometry was employed in the current study. It is well accepted that this tool may be used to describe the surface morphology and complexity of various materials.[11] A scale-dependent parameter named fractal dimension (D_f) is proposed to quantify the degree of surface roughness. Usually, the D_f value of thin films lies between 2 and 3. A smooth surface possesses D_f =2, and a higher D_f value suggests a rougher and space-filling surface.[12] However, to our knowledge, fractal geometry used in BPs characterization applications has not been reported yet until now.

In this scenario, we reported here for the first time the characterization of BPs using fractal analysis. The surface morphology of the BPs was characterized by scanning electron microscopy (SEM). The D_f values were then calculated based on the grayness distribution of SEM images, thus providing a new parameter in evaluating the performance of BPs. Consequently, it can be concluded that there exists a relation between D_f value and adsorption capability. For this reason, adsorption experiments were carried out. In addition, the results from nitrogen adsorption analysis were also presented for the sake of comparison. As expected, some new and important results were obtained and much effort had been made for their clarifications.

2. Experimental

2.1. Reagents and materials

High purity (over 99.5%) SWNTs and MWNTs were provided by Kanagawa Academy of Science and Technology (Japan), and their main properties were listed in Table 1. Considering that pretreatment of CNTs was critical for the preparation of BPs, the as-received CNTs were subjected to further acid treatment and heat annealing.[13] The acid treatment was conducted in 0.1 M HCl for 10 min, while the heat annealing was carried out in a vacuum oven (at pressure of 0.01 Pa) at 1700℃ for 20 min. Reagent-grade ethanol and humic acid (HA, in the form of sodium salt) were purchased by Wako (Japan).

2.2. Sample preparation

Buckypapers were prepared by sonication in 300 ml ethanol of up to 10 min to disperse 50 mg SWNTs or 50 mg MWNTs (both with pretreatment). Each suspension was then filtered using the dead end filtration through 0.45 μm PTFE membranes. CNT buckypapers were peeled directly from the PTFE membranes and dried in an oven (at 110℃) overnight.[14] Interestingly, it was found that these two BPs exhibited different film thickness and areal density (see Table 2).

2.3. Analytical apparatus and calculations

The surface morphology of the BPs samples was investigated using field emission scanning electron microscopes (FE-SEM, Zeiss Ultra Plus). The D_f values were then determined by the Triangular Prism Surface Area methodology of a Fractal Fox 2.0 program.[15] Noting that prior to the calculations, Laplacian filters must be applied to exclude any influences from the noise of the SEM images (the denoising regularization parameter was set as 1.0).[16] For comparison purposes, low-pressure nitrogen adsorption analysis was also employed to calculate the D_f values of the two samples,[17] which was done on a V-Sorb 2800S SI Surface Area Analyzer (Gold APP, Beijing, China). It had been well proved that the fractal FHH (Frenkel, Halsey, Hill) equation (Eq. (1)), was very suitable for application in the case of porous materials.[18]

$$\ln(V) = \boldsymbol{k} \ln(\ln(P_0/P)) + C \quad (1)$$

$$D_f = 3 + \boldsymbol{k} \quad (2)$$

where V was the volume of nitrogen adsorbed at each equilibrium pressure (ml/g); $\boldsymbol{k}$ was power-law exponent; P_0 and P were the saturation and equilibrium pressures of nitrogen, respectively (MPa); and C was the constant of gas adsorption.

2.4. Adsorption experiments

The as-prepared BPs were used as absorbents for HA removal from aqueous solutions. Adsorption experiments were conducted by batch mode in stoppered conical flask. All solutions were prepared by dissolving HA in deionized water (with initial concentration of 20 mg L^{-1}). For each time 50 mg BPs and 20 ml HA solution were mixed in the flask, which was then shaken in a thermostat shaker at 100 rpm. Note that all the adsorption experiments were carried out in triplicate, and results were reported as the mean with standard deviations. Samples were taken at preset time intervals and then analyzed by a UV-1800 spectrophotometer (Shimadzu, Japan) at λ_{max} 254 nm. The adsorption capability (Q) of BPs was calculated as follows (Eq. (3)):

$$Q = (c_0 - c)\, V/M \quad (3)$$

where c_0 and c were the concentrations of HA before and after the adsorption (mg L^{-1}), V was the volume of solutions (L) and M was the amount of BPs (mg).

3. Results and discussion

In Fig. 1 we illustrate the SEM images of the two tested BPs (SWNT-BP and MWBP) at different imaging areas (25~250000 μm^2).

From the micrographs, one may see that: 1) both BPs are self-supporting films, appearing as amorphous, rough and crack-free paper-like sheet; 2) a closer SEM examination reveals that the surface

of MWNT-BP is smoother than that of SWNT-BP; 3) for both cases, the individual nanotubes become visible at higher magnification view, which form a random, heavily interconnected macroporous system. Specifically, the network of SMNTs is much tighter than that of MWNTs.

The D_f values were then calculated from the SEM images and the results are presented in Table 3. Some phenomena may thus be observed:

(1) The microstructure of both BPs can be well described as being self-similar within a cutoff length scale. However, at lower scales (below 10 μm), the D_f values of both BPs are scale dependent. For instance, the D_f value of MWNT-BP drops from 2.582 to 2.398 as imaging area decreases from 2500 μm^2 to 25 μm^2. This is not surprising since the morphology of real materials can only be mapped into finite fractal;[19]

(2) For both cases, the mean D_f values obtained are quite high (2.5-2.8), revealing the high surface roughness of BPs. For BPs, higher surface roughness means larger active surface areas and higher adsorption capability.[20] Thus, the present result offers another essential explanation for the excellent performance of CNTs in decontamination processes;

(3) The mean D_f value of SWNT-BP (2.744) is higher than that of MWNT-BP (2.559), providing a rougher topography, so a better adsorption capability. This assumption is made because rough films may be advantageous for adsorbent that requires a large surface area.

To confirm the hypothesis, adsorption experiments with both BPs were conducted. Operating conditions being equal, the influence of reaction time on the adsorption of HA by these two BPs is depicted in Fig. 2.

Clearly, an exponential increase in adsorption of HA is registered within the first 60 min for both cases. Thereafter, a saturation plateau is reached. For an initial HA concentration of 20 mg L^{-1}, the adsorption capabilities of SWNT-BP and MWNT-BP are 4.3 mg g^{-1} and 3.0 mg g^{-1}, respectively. Please consider, the information from adsorption processes mainly reveals the interactions between adsorbed molecules (HA) and surface of films (BPs). Thus, we conclude that such difference may be explained by

the D_f values of each BPs, thus creating the link between macroscopic and microscopic behaviors. On the other hand, the results are also consistent with the inner structures of the samples. As shown in Fig. 3, there are marked differences between these two BPs. The most intriguing feature of SWNT-BP may be the macropores among the network, which may provide more adsorption sites for humic acid or nitrogen. The differing adsorption/desorption capability of the two BPs will also be appreciated in the isotherms from the following measurements (please refer to Fig. 4).

As mentioned previously, low-pressure nitrogen adsorption analysis had also been adopted to calculate the D_f values of both BPs. The nitrogen adsorption-desorption isotherms of the BP samples are shown in Fig. 4. The graph clearly evidences that SWNT-BP enables higher adsorption volume than MWNT-BP. It means that the adsorption capability of SWNT-BP is much higher than that of MWNT-BP. On the other hand, desorption of nitrogen at SMNT-BP is more difficult than that at MWNT-BP. One possible explanation is that, most layers in MWNTs cannot adsorb anything as they are sandwiched between other graphitic layers, which in turn only add up extra mass without contributing to surface area. While for the case of SWNTs, all graphitic layers contribute to adsorption naturally, and the adsorption may even occur in the cavity of individual nanotubes.[21]

The plots of $\ln(V)$ vs. $\ln(\ln(P_0/P))$ of the two BPs according to FHH equation are shown in Fig. 5, both revealing excellent linearity ($R^2 > 0.90$). The D_f values determined from such analysis are 2.656 and 2.462 for SWNT-BP and MWNT-BP, respectively. Comparing the samples of SWNT-BP and MWNT-BP, the D_f value of the former is still higher than that of the latter, confirming that the pore structure of SWNT-BP is more complicated.[17] In this light, the diffusion, percolation and desorption of molecules in SWNT-BP are more difficult than those in MWNT-BP. In this light, this D_f value may be used to characterize the complexity of pore structures in buckypapers. Returning to Table 2, clearly for both cases, the D_f values calculated from SEM imaging are higher than those from nitrogen adsorption analysis. This is not surprising since these two different D_f values of each BPs are obtained from

multi-scale and single scale analyses, respectively. Despite this, the surface roughness of BPs still plays the major role in adsorption process, especially in the case of big molecules such as humic acid.[3,14]

As a result, the BPs characterization with fractal analysis contributes to the understanding of the surface morphological characteristics and pore structures. Although the surface and inner structures of BPs are far from entirely understood, the results reported here demonstrate a novel tool in evaluating their performances.

4. Conclusions

In this work, we have initially explored the surface morphology of buckypapers using fractal concepts. By this approach a quantitative characterization of surface morphology can be achieved, thus leads to new dimension of understanding how the surface properties of BPs are influenced by the nature of CNTs. Specifically, it has been found that SWNT-BP exhibits higher D_f value than MWNT-BP, revealing different surface roughness and pore structure. Considering that the properties of BPs are also strongly dependent on the preparation and purification technology of CNTs, extensive research works are thus recommended to be forward in this field.

FIGURE & TABLE CAPTIONS

Fig. 1. SEM images of SWNT-BP (the 1st column) and MWNT-BP (the 2nd column) at different imaging areas

Fig. 2. Adsorption kinetics of HA onto SWNT-BP and MWNT-BP (initial HA concentration: 20 mg L^{-1}, adsorbent dosage: 50 mg and at 25 ℃)

Fig. 3. Cross-section structure of SWNT-BP (a) and MWNT-BP (b)

Fig. 4. The nitrogen adsorption-desorption isotherm of the BP samples

Fig. 5. Plots of ln(V) vs. ln(ln(P_0/P)) reconstructed from the nitrogen adsorption data

Table 1. The properties of SWNTs and MWNTs

Table 2. The film thickness and areal density of the prepared SWNT-BP and MWNT-BP

Table 3. The fractal dimensions of BPs versus different imaging areas of SEM images

Acknowledgments

The work described in this paper is supported by Fundamental Research Fund for the Central Universities, Nanjing Agricultural University (KJQN201551).

REFERENCES

1 Y. Liu, Y. Zhao, B. Sun and C. Chen, *Acc. Chem. Res.*, 2013, **46**, 702-713.

2 Y. Zhou, S. Shimada, T. Saito and R. Azumi, *Carbon*, 2015, **87**, 61-69.

3 O. G. Apul and T. Karanfil, *Water Res.*, 2015, **68**, 34-55.

4 O.G. Apul, Y. Zhou and T. Karanfil, *J. Hazard. Mater.*, 2015, **295**, 138-144.

5 W. Sun, B. Jiang, F. Wang and N. Xu, *Chem. Eng. J.*, 2015, **264**, 645-653.

6 H. Kim, Y. S. Hwang and V. K. Sharma, *Chem. Eng. J.*, 2015, **255**, 23-27.

7 C. Jung, J. Heo, J. Han, N. Her, S. Lee, J. Oh, J. Ryu and Y. Yoon, *Sep. Purif. Technol.*, 2015, **106**, 63-71.

8 M. H. Rashid, S. Q. T. Pham, L. J. Sweetman, L. J. Alcock, A. Wise, L. D. Nghiem, G. Triani, M. Panhuis and S. F. Ralph, *J. Membrane Sci.*, 2014, **456**, 175-184.

9 J. G. Park, S. Li, R. Liang, C. Zhang and B. Wang, *Carbon*, 2008, **46**, 1175-1183.

10 J. Zhang and D. Jiang, *Compos. Part A: Appl. Sci.*, 2012, **43**, 469-474.

11 M. Schroeder, *Fractals, Chaos, and Power Laws: Minutes from an Infinite Paradise*, Dover Publications, New York, 2009.

12 S. Kulesza and M. Bramowicz, *Appl. Surf. Sci.*, 2014, **293**, 196-201.

13 J. W. Jang, K. W. Lee, C. E. Lee, B. Kim and C. J. Lee, *Curr. Appl. Phys.*, 2013, **13**, 1069-1074.

14 X. Yang, J. Lee, L. Yuan, S. Chae, V.K. Peterson, A. I. Minett, Y. Yin and A. T. Harris, *Carbon*, 2013, **59**, 160-166.

15 C. Zhang, J. Wu and D. Fu, *Appl. Surf. Sci.*, 2014, **313**, 750-754.

16 S. Dhillon and R. Kant, *Appl. Surf. Sci.*, 2013, **282**, 105-114.

17 X. Liu, J. Xiong and L. Liang, *J. Nat. Gas Sci. Eng.*, 2015, **22**, 62-72.

18 Y. Yao, D. Liu, D. Tang, S. Tang and W. Huang, *Int. J. Coal Geol.*, 2008, **73**, 27-42.

19 R. P. Yadav, S. Dwivedi, A. K. Mittal, M. Kumar and A. C. Pandey, *Appl. Surf. Sci.*, 2012, **261**, 547-553.

20 J. M. Sieben, A. Anson-Casaos, M. T. Martinez and E. Morallon, *J. Power Sources*, 2013, **242**, 7-14.

21 G. Chen, X. Shan, Y. Wang. Z. Pe, X. Shen and B. Wen, *Environ. Sci. Technol.*, 2008, **42**, 8297-8302.

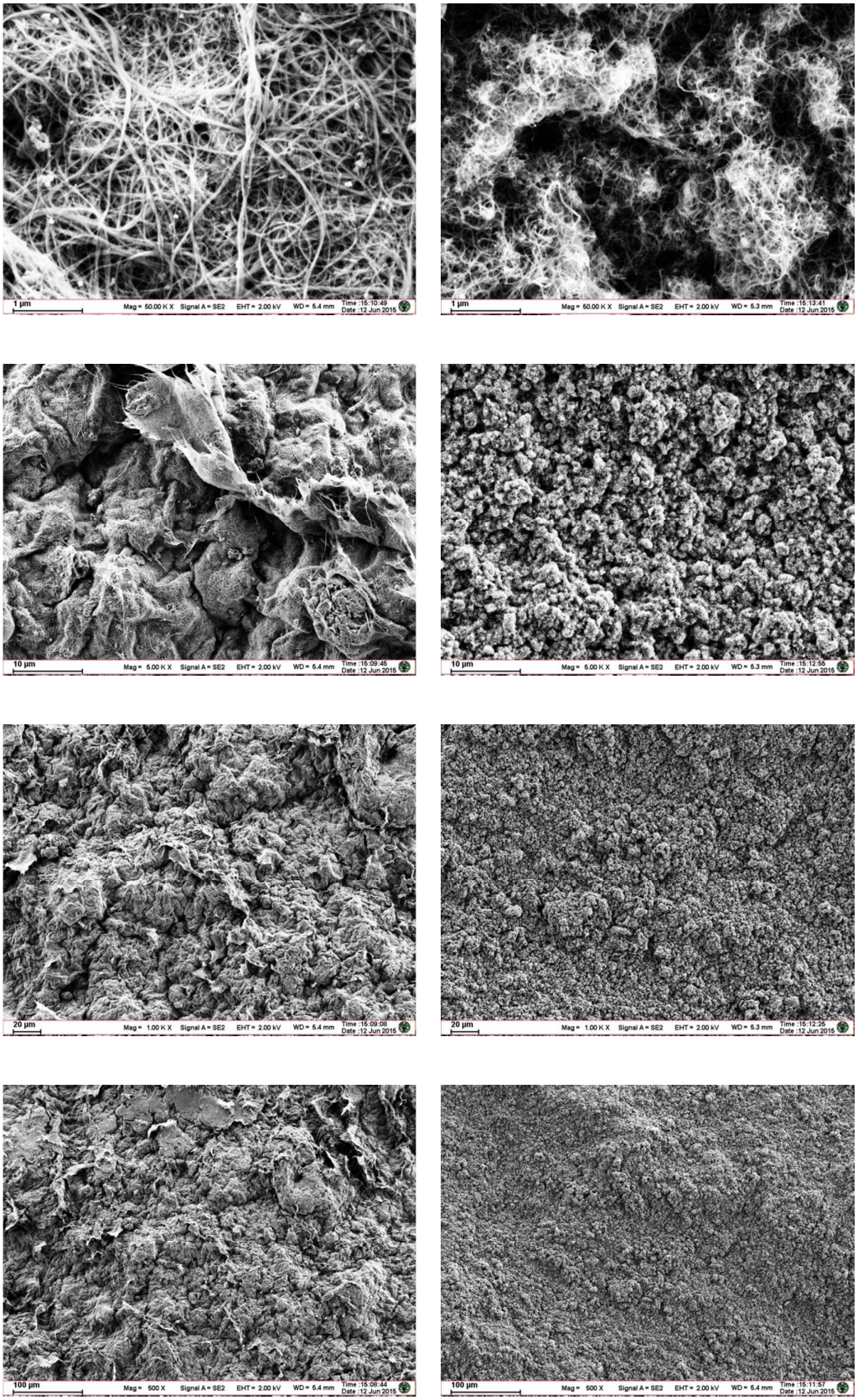

Fig. 1

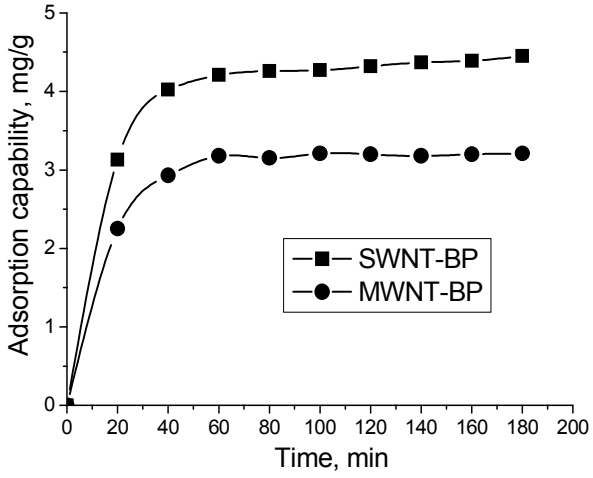

Fig. 2

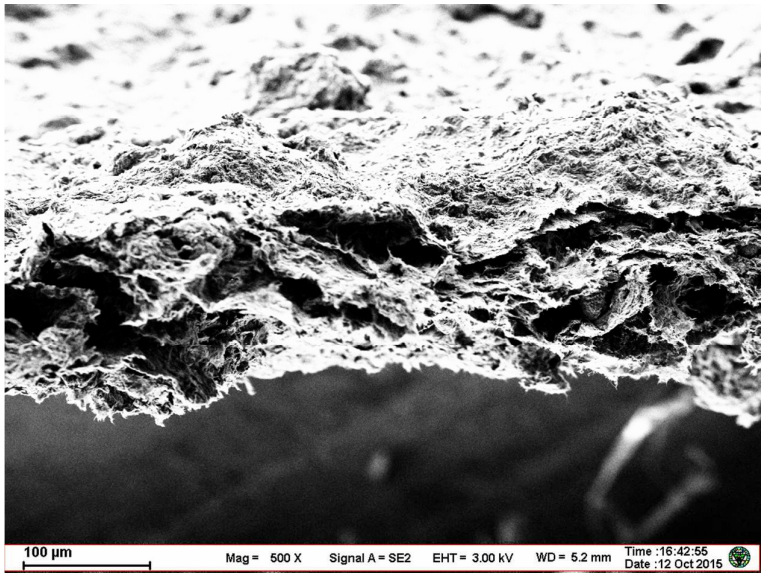

(a)

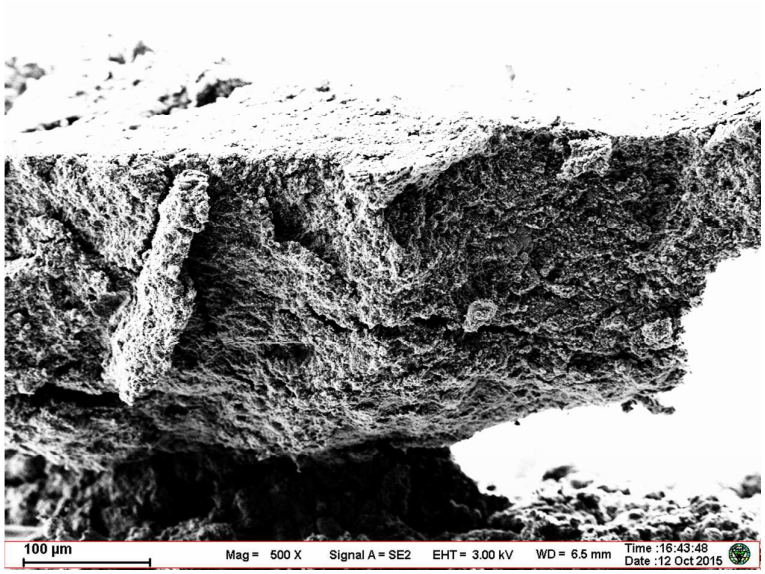

(b)

Fig. 3

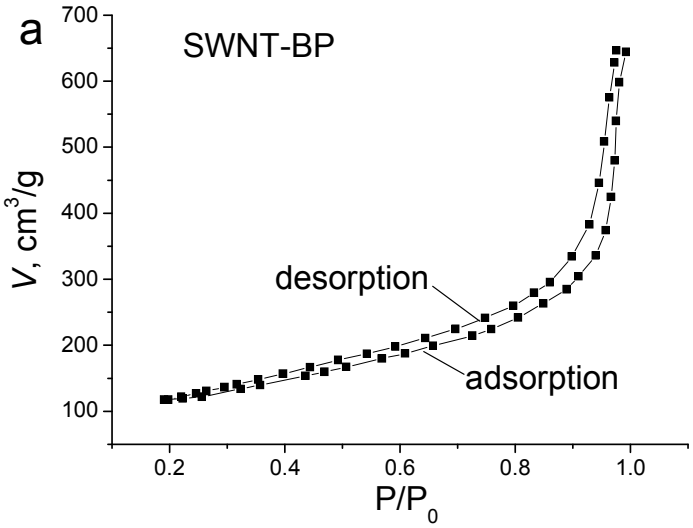

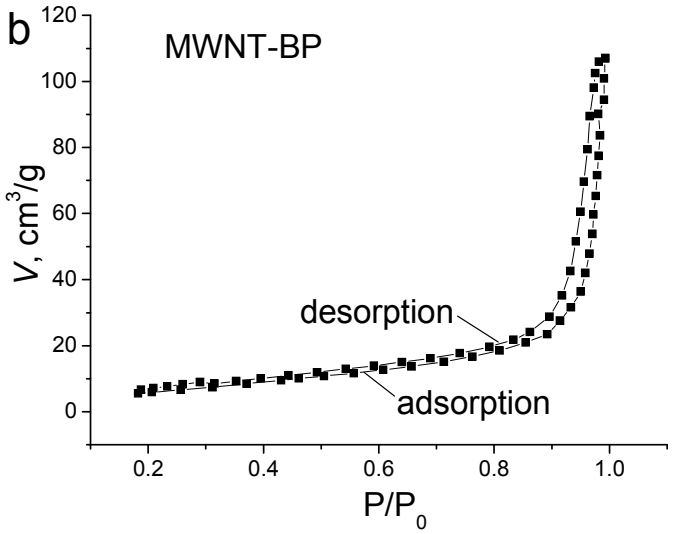

Fig. 4

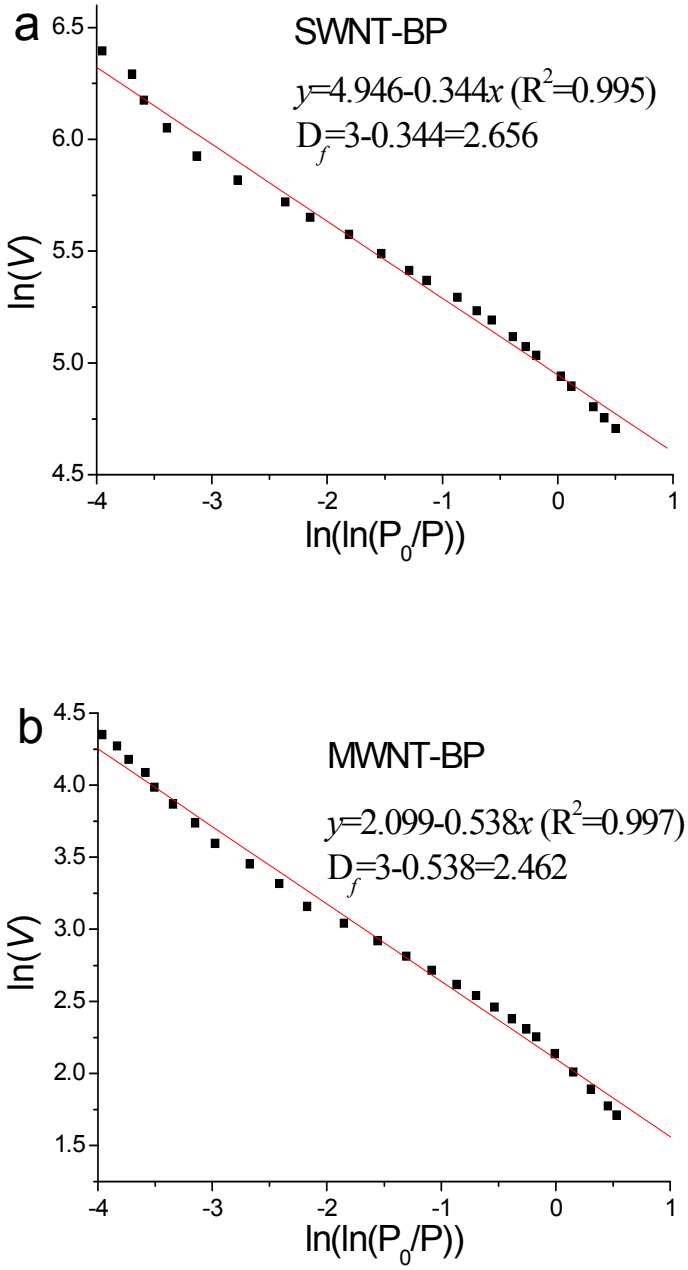

Fig. 5

Property	SWNTs	MWNTs
Outer diameter	1.5 nm	8~13 nm
Length	5~30 μm	8~10 μm
BET surface area	320 $m^2 g^{-1}$	140 $m^2 g^{-1}$
Conductivity	100 S cm^{-1}	77 S cm^{-1}

Table 1

Property	SWNT-BP	MWNT-BP
Film thickness	125±10 μm	216±16 μm
Areal density	16.76 mg/cm^2	24.35 mg/cm^2

Table 2

Imaging Area	25 μm^2	2500 μm^2	62500 μm^2	250000 μm^2	mean value
SWNT-BP	2.689	2.710	2.785	2.791	2.744
MWNT-BP	2.398	2.582	2.630	2.627	2.559

Table 3

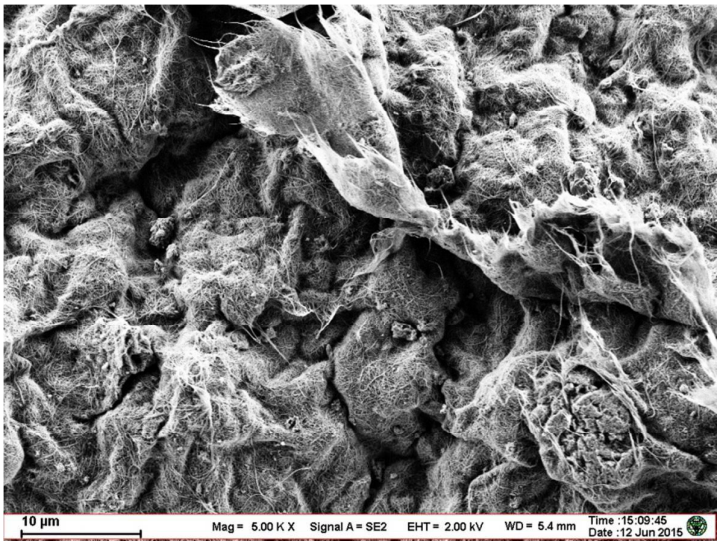

Buckypapers made of SWNTs

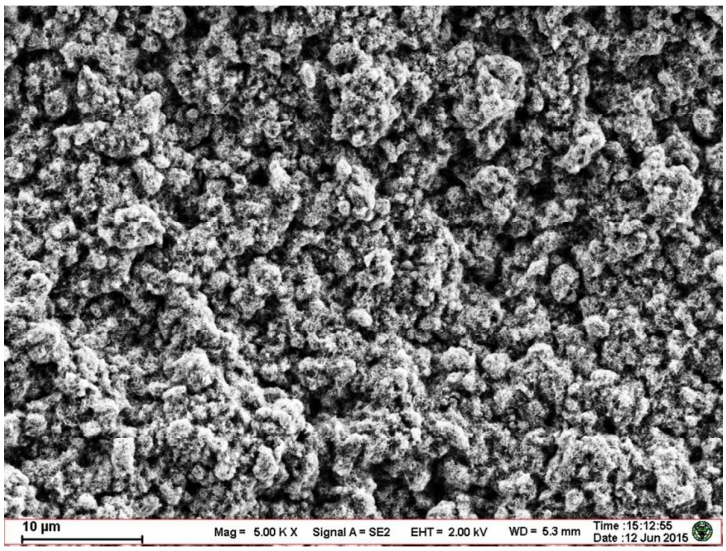

Buckypapers made of MWNTs